Towards self-powered sensing and thermal energy harvesting in high-performance composites via self-folded CNT honeycomb structures

*Kening Wan,[a] Arnaud Kernin,[a] Leonardo Ventura,[a] Chongyang Zeng,[a] Yushen Wang,[a] Yi Liu,[a,b] Juan J. Vilatela,[c] Weibang Lu,[d] Emiliano Bilotti,[a,e,**] Han Zhang[a,*]*

a. School of Engineering and Materials Science, Queen Mary University of London, Mile End Road, London E1 4NS, UK

b. Department of Materials, Loughborough University, Loughborough LE11 3TU, UK

c. IMDEA Materials Institute, Eric Kandel 2, 28906, Getafe, Madrid, Spain

d. Division of Advanced Nanomaterials and Innovation Center for Advanced Nanocomposites, Suzhou Institute of Nano-Tech and Nano-Bionics, Chinese Academy of Sciences, 215123, PR China

e. Department of Aeronautics, Imperial College London, Exhibition Road, London, SW7 2AZ, UK

* Corresponding authors: han.zhang@qmul.ac.uk e.bilotti@imperial.ac.uk

KEYWORDS: thermoelectric, carbon nanotubes, temperature induced self-folding, self-powered sensing

ABSTRACT

The development of high performance self-powered sensors in advanced composites addresses the increasing demands of various fields such as aerospace, wearable electronics, healthcare devices, and the Internet-of-Things. Among different energy sources, the thermoelectric effect which converts ambient temperature gradients to electric energy is of particular interest. However, challenges remain on how to increase the power output as well as how to harvest thermal energy at the out-of-plane direction in high-performance fiber reinforced composite laminates, greatly limiting the pace of advance in this evolving field. Herein, we utilize a temperature induced self-folding process together with continuous carbon nanotube veils to overcome these two challenges simultaneously, achieving a high thermoelectric output (21mV and 812 nW at temperature difference of 17 ºC only) in structural composites with the capability to harvest the thermal energy from out-of-plane direction. Real-time self-powered deformation and damage sensing is achieved in fabricated composite laminates based on a thermal gradient of 17 ºC only, without the need of any external power supply, opening up new areas of autonomous self-powered sensing in high-performance applications based on thermoelectric materials.

1. Introduction

Thermoelectric (TE) modules consist of alternating p-n legs can convert thermal energy from ambient environments to electric energy, allowing to power up existing modules without needing external power supply or batteries. This is particularly attractive in many fields like wearable electronics, robotics, wireless sensors, and high-performance composite materials, especially those

systems in remote or hard to access locations where reliance on external batteries should be minimized.

Compared with various organic TE materials such as derives of poly(3,4-ethylenedioxythiophene) (PEDOT) and poly(3-hexylthiophene-2,5-diyl) (P3HT), carbon based (nano)materials have achieved rapid development with many promising results over last few years due to their relatively low cost and environmental sustainability. In particular, great research interests can be found in carbon nanotubes (CNTs) based TE materials thanks to their various self-standing assemblies such as fibers, yarns, veils, and fabrics available in large quantities via continuous production [1-2], allowing easy integration and fabrication alongside tuneable TE properties [3-5], high electrical conductivity [6-7], and potential mechanical reinforcement [8]. Ultrahigh power factor of 2482 μW m^{-1} K^{-2} [7, 9] and 3103 μW m^{-1} K^{-2}[10] at room temperature have been reported for both single-wall carbon nanotube (SWNT) and multi-wall carbon nanotube (MWNT) continuous films, respectively.

To achieve a high-power output from the TE device, a feasible route to connect p-type and n-type alternating legs is equally important to the high-performance TE material itself, which is sometime overlooked hence limits their practical applications. Only few attempts can be found in realizing p-n connection for CNT assembly-based TE devices. Zhou *et al.* [7] reported a compact-configuration flexible TE modules based on the vacuum filtrated CNT film, with a thermopower of 410 μV K^{-1} and maximum 2.51 μW power output achieved at ΔT~27.5 ºC at in-plane direction. Choi *et al.* [11] fabricated a flexible thermoelectric generator to harvest the thermal energy in out-of-plane direction by doping the continuous CNT yarns with alternating p-type and n-type around a polydimethylsiloxane (PDMS) block, with a maximum power density of 697 μW g^{-1} at ΔT~40 K

based on 90 pairs of p-n connections. Choi *et al.* [12] also demonstrated that with 9 pairs of p-n connections, the CNT films can generate 3.4 mV by converting body heat directly ($\Delta T \sim 7$ ºC).

In fact, only from the last year, a few efforts can be found in utilizing integrated TE modules in high performance lightweight structural applications where many waste heats are available. Paipetis' group presented a CNT painted glass fiber with the cost of either need in-plane temperature gradience [13] or only achieve single leg device [14]. In 2019 [15], Karalis *et al.* utilized a series of p-type and n-type doped commercial carbon fiber tows as bottom ply of a structural TE composite, with 5 pairs of p-n legs generating 19.56 mV voltage output at $\Delta T \sim 75$K from in-plane thermal gradient. Very recently, Karalis *et al.* used CNT inks to coat on glass fiber fabrics and built 8 pairs of p-n layers alternating between insulating glass fibers, achieving power output of 2.2 μW at ΔT of 100K from in-plane thermal gradient. Although the feasibility of integrating TE modules into structural composites has been successfully demonstrated, it is worth noting that many of the thermal gradients in fiber reinforced composite applications are found at out-of-plane (through thickness) direction.

Clearly, to utilize the TE effect in nano-engineered high-performance composites, two obvious and practical challenges remain: (i) how to utilize the out-of-plane thermal gradient, since most of the thermal gradients exist across the thickness direction of the components rather than in-plane; (ii) how to increase the power output from TE modules, or in other words, how to effectively connecting the alternating p-g legs. Another key design criterion for any nano-engineered composites is the integration of system without significantly affecting the original performance while adding new functionalities.

Herein, we present an innovative strategy to achieve high power output TE in structural composites, addressing all three challenges simultaneously by utilizing a Kirigami inspired self-

folding process to establish a CNT film-based honeycomb structure. The well acknowledged mechanically robust honeycomb structure can enable not only the utilization of thermal gradient along the out-of-plane direction, but also capability for alternating p-n legs to be well connected for energy harvesting. The electrical power output obtained from this integrated TE honeycomb in hierarchical composites is sufficient to perform the *in-situ* deformation and damage sensing, providing added multi-functionalities such as self-powered structural health monitoring. This new method to integrate TE module into hierarchical composites via self-folding to form honeycomb structure could be used in various high performance composite applications in the fields of aerospace, automotive and renewable (solar) energy sectors, especially at remote and hard to access locations.

2. Material and Methods

2.1 CNT veils fabrication

CNT veils were made by floating catalyst chemical vapor deposition (FCCVD) method. The feedstock consists of about 96.5 wt.% ethanol (carbon source), 1.9 wt.% ferrocene (catalyst precursor) and 1.6 wt.% thiophene (promoter), was injected (at the rate of 0.15 ml/min) into a CVD furnace (~1150 ºC) along with the carrier gas (at the rate of 600 ml/min) of hydrogen and argon (ca. 1:1 in volume). Detailed fabrication procedures can be found in previous publications[16-17]. The CNT were formed and entangled into sock-like aerogel in the furnace, then was pulled out and collected by a rotating roller continuously. As a result, the high porosity CNT sponge on the roller was half densified by mechanical compression and followed by the annealing-acid wash procedure.

The ‘as-grown’ CNT for veils has been anealled at 450 ºC in air for one hour then immersed in hydrochloric acid (36 % ~ 38 %) for 12 hours. Afterwards, the CNT veils has been washed in deionized water seveal times until the pH value reaches 6~7, then dried in the oven at 100 ºC for 2 hours before testing and doping.

Polyethylenimine (PEI) and $FeCl_3$ were dissolved in ethanol and used for n- and p-type doping, respectively. Different concentrations of the dopant solutions have been used ranging from 2 mM to 20 mM. For comparison, the amount of the dopant solutions are all kept 50 µl, and dropped onto a 15mm×15 mm squared CNT veils on glass slide substrates.

2.2 Self-folding TE module structures and fabrication

250 µm thickness PC film (LEXAN™ 8010 Film) is provided by SABIC. Three types of the PC patches: small (8mm×1.5mm), medium (8mm × 8.5mm) and large (8mm ×10mm) have been cut by Silhouette cameo. A commercial bi-oriented Polystyrene film (Grafix shrink film) were cut into the designed patterns. CNT veils were cut into the same patterned as the b-PS and then densified by a few drops of ethanol in order to adhere CNT onto both sides of the b-PS film. After the doped CNT veils being dried at 40 ºC, cyanoacrylate glue (Loctite®, Henkel Ltd.) was used to adhesively bond the CNT veils onto b-PS substrate and PC patches. The as-assembled sample was then dried at room temperature overnight, before placing into the 130ºC oven for self-folding processes.

2.3 Self-powered nano-engineered composite laminates

A total of 60 mg of carbon nanotubes (NC7000, Nanocyl S.A.) were dispersed in acetone by probe sonication with 5000 J energy at 20% of the maximum amplitude level. The spray coating was performed using an airbrush (H4001 HP-CPLUS, Iwata Performance) connected to the air compressor (Iwata studio series) to deposit CNTs onto the surface of a 10 × 10 cm twill glass fiber/epoxy prepreg (MTC510 from SHD Composites). It is worth mentioning that the electrically

insulating glass fiber reinforcement has been chosen for this work in order to avoid the electrical short connections between the plies. 30 psi (2.07 bar) air pressure and a 10 cm distance between spraying nozzle and prepreg were used as our previous study[18-19]. The measured 60 mg of CNTs were spray coated onto the top surface of prepreg, resulting in ~ 7 wt.% CNT loading to the resin. The CNT coated prepreg was then placed on top of another four piles of uncoated prepregs, with the coated surface facing up as the outer conductive layer. After degassed under vacuum for 30 minutes to avoid any trapped air, a curing cycle of 120 °C for 2 h with heating rate of 3 °C/min from room temperature was employed with an active vacuum applied throughout. Thin copper wires were used as electrodes to connect the TE module and sensing surface of the fabricated composite laminates.

2.4 FEM modelling

A multi-physics FEM model in Abaqus was used to model the self-folding process. A first transient heat-transfer simulation to reproduce the composite heating was used as the input for the thermal properties of the materials and the external temperature. The efficiency of the heat transfer has been adjusted to match the experimental results. The dynamic model for reproducing the self-folding behavior of the structure is based on an explicit formulation with the input of the simulated temperature profile. The temperature profile is assumed to be homogeneous inside of the geometry due to its low thickness. The large strains taking place in the active material due to the temperature change led to mesh distortion issues, so an adaptive mesh and a fine discretization in time are required.

2.5 Characterization

Two-probe method has been used to measure and compare the resistance change before and after folding for CNT specimens. A bespoke four-point probe system consisting of an Agilent 6614

System DC power supply, a Keithley 6485 picometer and a Keithley 2000 multimeter, was used for electrical conductivity of as-fabricated and doped CNT veils with a probe space 0.25 mm. The thickness of the as fabricated and doped CNT veils was measured by Bruker Dektak Vision 64 profilometer. The Seebeck coefficient was measured at 27 ºC under nitrogen atmosphere, using the MMR Technology Seebeck Effect Measurement System.

The folding angle of the samples were recorded by taking the live videos from the side views at 120 ºC, then analyzed by Image J software. The infrared camera (FLIR E40) was used to monitor the temperature gradient between two sides of laminates, with temperature analysed by the FLIR software. Scanning electron microscope (SEM, FEI Inspect F) was used to examine the morphology of samples, with 3 kV accelerating voltage used. The thermal stability was characterized through thermogravimetric analysis (TA Instruments Q500) with applied temperature from 20 ºC to 900ºC at the rate of 10 ºC min^{-1} in air, with isothermal steps of 10 min at both the start and the final temperatures. The Raman spectra were collected from an inVia Qontor confocal Raman microscope with a 633 nm laser source for 5% power under 50× magnification.

Subjected to a given temperature gradient, the open circuit voltage of the self-folded module was measured directly by a Keithley 2000 multimeter. For the power output measurements, a variable resistor was connected to the self-folded TE module. Voltage and current were recorded simultaneously by a voltmeter (Keithley 2000 Multimeter) and a picoammeter (Keithley 6485) with the resistor change from 0 Ω to 999 MΩ. The maximum power output can be obtained when the resistance of the load equals to the inner resistance of the module.

For the *in-situ* damage sensing tests, the electrical resistance change of the composite panel was recorded by an Agilent 34401A 6½ digital multimeter during the three point bending tests. A

picoammeter (Keithley 6485) was used to record the current output generated from the honeycomb TE module in real time under the temperature difference of 17 ºC for the self-powered sensing setup. Silver paints were used to eliminate the contact resistance between specimens and electrodes. All three point bending tests were performed in accordance with ASTM D790, with the sample dimensions of 12.7mm × 85 mm × 3 mm.

3. Results and Discussions

3.1 Thermoelectric performance of CNT films

The thermoelectric properties of CNT films have been systematically characterised, with annealing and purification processes employed to improve their performance. The effect of subsequent folding steps on the electrical properties has also been examined. A large sized CNT veil (1.5 m^2) has been manufactured by a floating catalyst based chemical vapor deposition (FCCVD) method. Since the thermoelectric property of CNT veils can be affected by the residual impurities such as metal catalysts and amorphous carbon from the manufactuing processes, annealing process at 450°C in air environments has also been employed in order to remove organic impurities.

Both the electrical conductivity and Seebeck coeffiecient (**Figure 1a**) have been significantly improved by applied annealing processes. The electrical conductivity trippled from 598 S cm^{-1} to 1878 S cm^{-1}, and Seeback coeffcient increased from 34 μV K^{-1} to 42 μV K^{-1}. This is attributed to the successful removal of the amorphous carbon by the annealing processes. It is well acknowledged that CNT veils can absorb oxygen and/or moisture from the environments, resulting in the formation of hole-like carriers acting as a p-type dopants [20] hence an increasing trend of p-type thermoelectric property after several days of exposure to the environments. For example the

as-grown CNT veil's Seebeck coefficient increase from 34 μV K^{-1} to 47 μV K^{-1} (**Figure S1**) exposed in air (1 atm, 25–27 °C, relative humidity of 65%) for 200 days. However this inflated value is unstable and varies depending on the environment. For example, with the high temperature temperarily absorbed oxygen and/or moisture being removed its Seebeck coefficient will reduce back (**Figrue S2**). Therefore, p-type doping is still necessary to maintain the CNT veil a stable seebeck coefficient and power factor under different situations. In the meantime, the Seebeck coefficient values in **Figure 1a** and **1b** were measured after at least 72 hours of the treatment and under the vacuum for 30min to ensure the consistent and reliable results, eliminating these potential influences.

Although an additional step of purification by acid washing can further improve the TE performance of CNT veils (seebeck coefficient further increase to 60 μV K^{-1} with a power factor reach to 1000 μW $m^{-1}K^{-2}$), the condensed veil network has inevitably impeded the subsequent doping process (**SI section 1** and **2**). Therefore, the doping of annealed CNT veils (without further acid washing) were successfully achieved by using $FeCl_3$ and PEI, with optimized Seebeck coefficient of 60 μV K^{-1} for p-type and -70 μV K^{-1} for n-type, respectively. Their electrical conductivity remained at same level after doping process, leading to an enhanced power factor of 688 μW $m^{-1}K^{-2}$ and 741 μW $m^{-1}K^{-2}$ for p-type and n-type at room temperature respectively (**Figure 1a**). The TE property is comparable to the literatures as summariesed in Table 1. As shown in **Figure 1b**, the stability of Seebeck coefficient has also been improved after performed doping process, with no obvious changes after 7 months in normal environments.

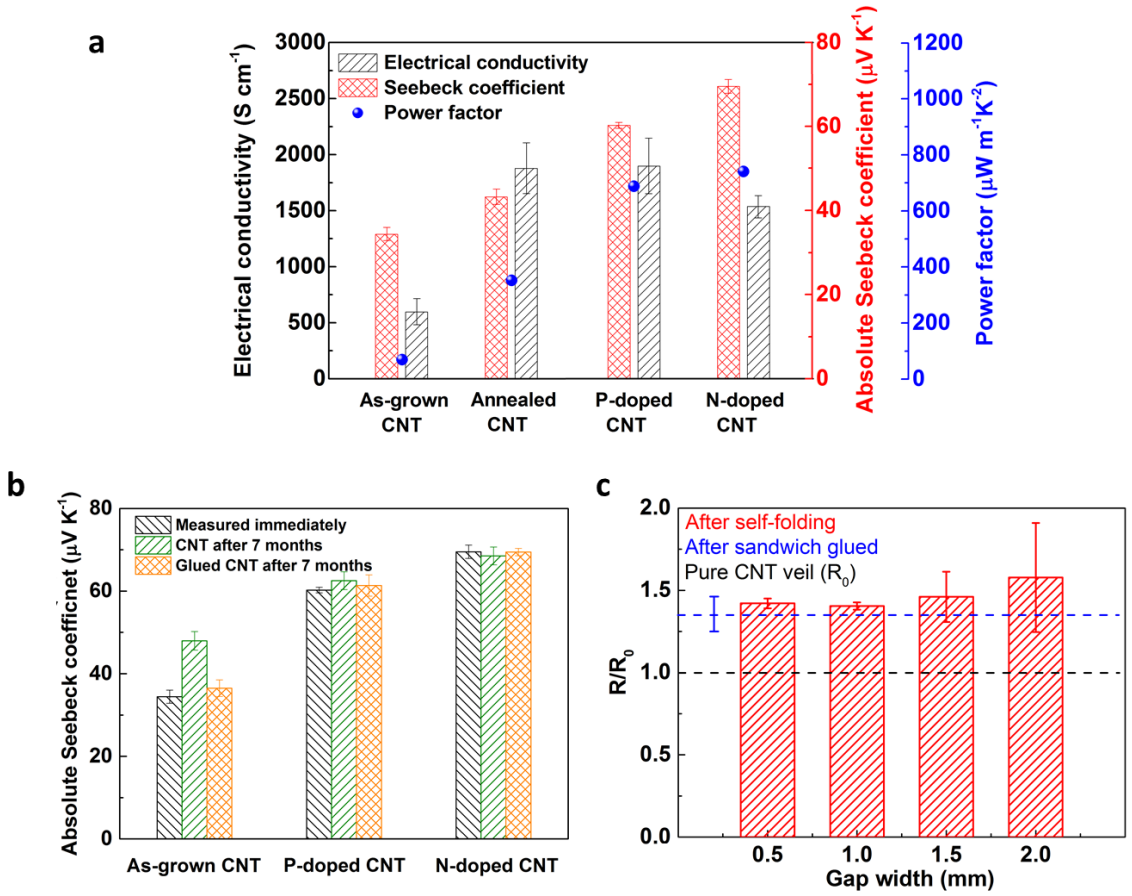

Figure 1. Thermoelectric properties of CNT veils. (a) The electrical conductivities, Seebeck coefficients and power factor of the as-grown, annealed, purified (acid-washed after annealed) and p&n doped CNT veils at room temperature, with improved properties after annealing processes. (b) Seebeck coefficients of as-grown, p and n doped CNT veils change in 7 months and the effect of the glue, indicating a stable TE performacne from current CNT films. (c) Effect of glue and folding processes on the electrical resistance of CNT veils, showing a slightly increased resistance value after applying glue and subsequent folding.

Table 1. TE property summary of the CNT based materials and corresponding TE generators

Materials	σ **(S cm^{-1})**	α **(μV K^{-1})**	**PF (μWm^{-1}K^{-2})**	**Ref**
This work	1878; 1500	60; -70	688; 741	
Doped CNT fibres wrapped with acrylic fibres	950	−64	330	[21]
CNT fiber	3000	90	2,500	[9]
Au-doped CNT webs	1090-5134	80	3548	[22]
$NaBH_4$ doped CNT film	2000	-80	1280	[23]
PEI doped CNT	600	-58	201	[5]
CNT with PEDOT:PSS	1300	-35	160	[24]
CNT yarns	3147	50; -31	160	[11]
Single-walled CNT buckypapers	600	-38	90	[26]
Carbon fiber composites	1630	33.85; −11.83	186; 22.8	[15]
PEDOT:PSS/CNT composite yarn	1043	70.1	512.8	[27]
CNT fiber	1899	26.7	432	[28]
CNT fiber	52	-86	40	[29]
CNT fabric	200	47.8; -49.1	40	[30]

To ensure a consistent and reliable electrical and TE performance of the CNT veils after subsequent fabrication and deformation in structural composites, the effect of deformation (folding) and employed adhesive in subsequent processes have also been examined (**Figure 1b** and **1c**). As expected, with the electrically insulating cyanoacrylate used as glue, CNT composites have shown a ~ 30% resistance increase compared with the pristine CNT veils of the same dimensions (blue dash line in **Figure 1c**). However, no change in the Seebeck coefficient values was found (**Figure 1b**). It is also worth noting that the insulating cyanoacrylate encapsulated the CNT veils to further avoid the oxygen absorption, ensuring a stable Seebeck coefficients after a long period of exposure (7 months) for the long-term stability and reliability of the fabricated devices. **Figure 1c** shows the increase in electrical ressitance due to the deformation of CNT veils from flat (0°) to a small angle (150° - 180°) during the folding process, with only limited changes in resistance values from encapsulated CNT specimens regardless of the gap width in folding structures.

3.2 Design and fabrication of engineered modular structure for CNT honeycombs via temperature induced self-folding process

Although the honeycomb structure is well developed as the core layer for sandwich structural applications, the folding process to turn the two-dimensional (2D) flat CNT veils into three-dimensional (3D) honeycomb modules with accurately connected alternating p-n legs remains a complex and challenging task. As mentioned earlier, a Kirigami inspired self-folding process is utilised in this work to achieve a honeycomb-structured thermoelectric module which can harvest the thermal energy from out-of-plate direction with connected p-n legs.

Inspired by our recent work [31], a bi-stretched polystyrene film (b-PS) was used as an active layer with the capability to shrink upon heating, together with a polycarbonate (PC) layer adhered on top acting as substrates and hinges to restrict the thermal shrinkage hence achieving the temperature induced folding process. As shown in **Figure 2a**, two thin layers of CNT veils (3~5μm individually) were used to sandwich the shrinkable b-PS layer adhesively, with the PC layer adhered at the outside (either top or bottom) of CNT/b-PS/CNT structures. By changing the location and patterns of intact PC layer, various shapes and dimensions can be programmed and achieved by the temperature induced self-folding processes. In order to understand the self-folding mechanism hence utilising this method to turn 1D CNT veils into 3D honeycomb structure with an accurate p-n leg connection, different designs have been examined as well (D1-3 in **Figure 2a**). To establish the folding profile and relationship between folding angles with time and temperature, a simple design (D1), as illustrated in **Figure 2b,** has been employed (**Figure 2c & Figure S8**). Upon increased temperature in the first 10s, the multi-layered design D1, first went through a slight opening of the hinge (up to −5°). As the sample was reaching the glass transition temperature of PS (around 110 ºC as shown in **Figure S8a**), a minor expansion of PS (about 0.1%) occurred. Then the sample started folding at time ≈ 12s, until reaching a maximum point. At this stage, the release of local stresses of the oriented PS molecular chains led to the contraction of b-PS layer (max. 50%), while the PC layers remained intact and constrained the shrinkage of PS layer, creating the torque at the hinges and generating the bending moment for the folding process. Very short response time (between 10 and 30s) was required for this temperature induced self-folding process, with a great programmability in both folding angles (ranging from 150° - 180°) and folding speed by tuning the gap width between intact layers (**Figure S8b**). This folding process has also been simulated by the finite element method (FEM) modelling (**Figure 2d & Video S1**) and fit well

with the experimental results (**Figure S9**). After optimising the gap width and designs with the aim of achieving the correct angles required for honeycomb structures (**Figure S8c,d**), D2 with gap width of 0.5 mm and D3 with gap width of 1 mm were employed to create the folding angle of 60^{o} and 180^{o} for honeycomb structures, respectively. As shown in **Figure 2e**, the p and n doping has been employed prior to the folding process, with the patterns suit the honeycomb shape with p-n legs connected autonomously for thermoelectric energy harvesting. The single modular honeycomb structure consists of one unit cell can be self-folded at 130 ^{o}C within a minute, with the sequential folding of D3 followed by D2 as demonstrated in **Figure 2e**.

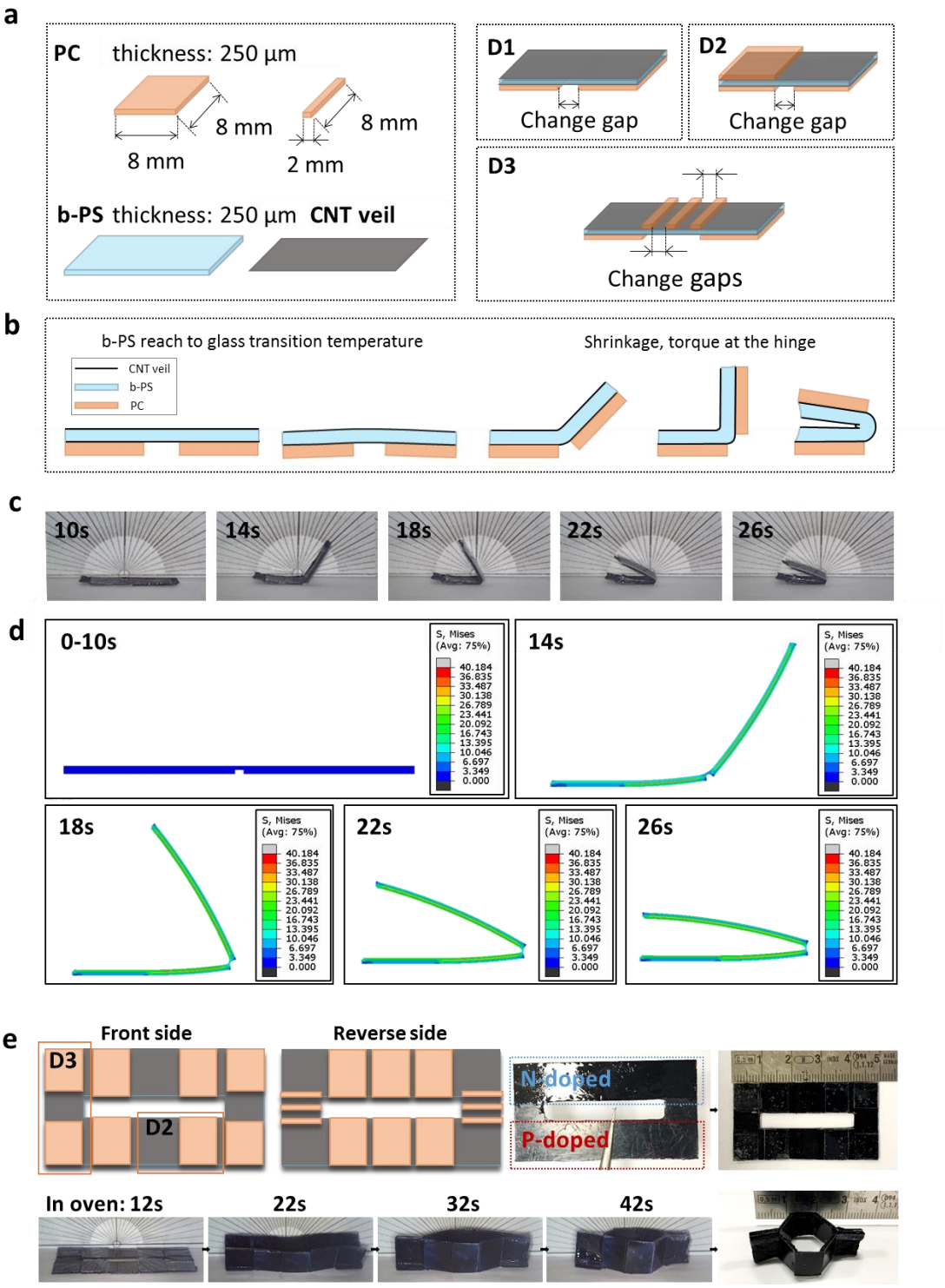

Figure 2. Engineered modular structure of self-folded honeycomb via temperature induced self-folding processes. (a) The schematic illustrations of three structure designs (D1-3) assembled by CNT veils, b-PS and PC. (b) The schematic illustrations of the self-folding process for D1. (c)

Images taken at different times of the self-folding process of D1 with gap width of 1mm, showing the folding angles as the function of time at 130 ºC. (d) Finite element method analysis of design D1 with the local stress values. (e) The designs and patterns for the modular unit cell honeycomb structure TE module, with circled areas of D2 and D3; and the images of self-folding processes at different stages.

To demonstrate the feasibility of utilising this self-folding process for high TE power output, a honeycomb structure consisting of four-unit cells has been fabricated. Benefitted from the formation of 4 pairs of alternating p-n legs on each side of patterned b-PS layer, 8 thermocouples have been achieved in this self-folded 4-cells honeycomb TE module (**Figure 3 & Figure S10**). Similar to the doping pattern of single module, the undoped regions (Figure 3a connected CNT veil) were folded to both sides of the module and acting as the electrodes to minimize the internal resistance of the fabricated TE module. The resistance of a 4-unit cell TE module is 12 ohm, which can be attributed to the continuous CNT veils with tailored patterns. Clearly, the vertical alignment of alternating p-n CNT legs in these fabricated TE modules can enable the thermal energy harvesting from the out-of-plane thermal gradients autonomously, opening up a much wider field of practical applications.

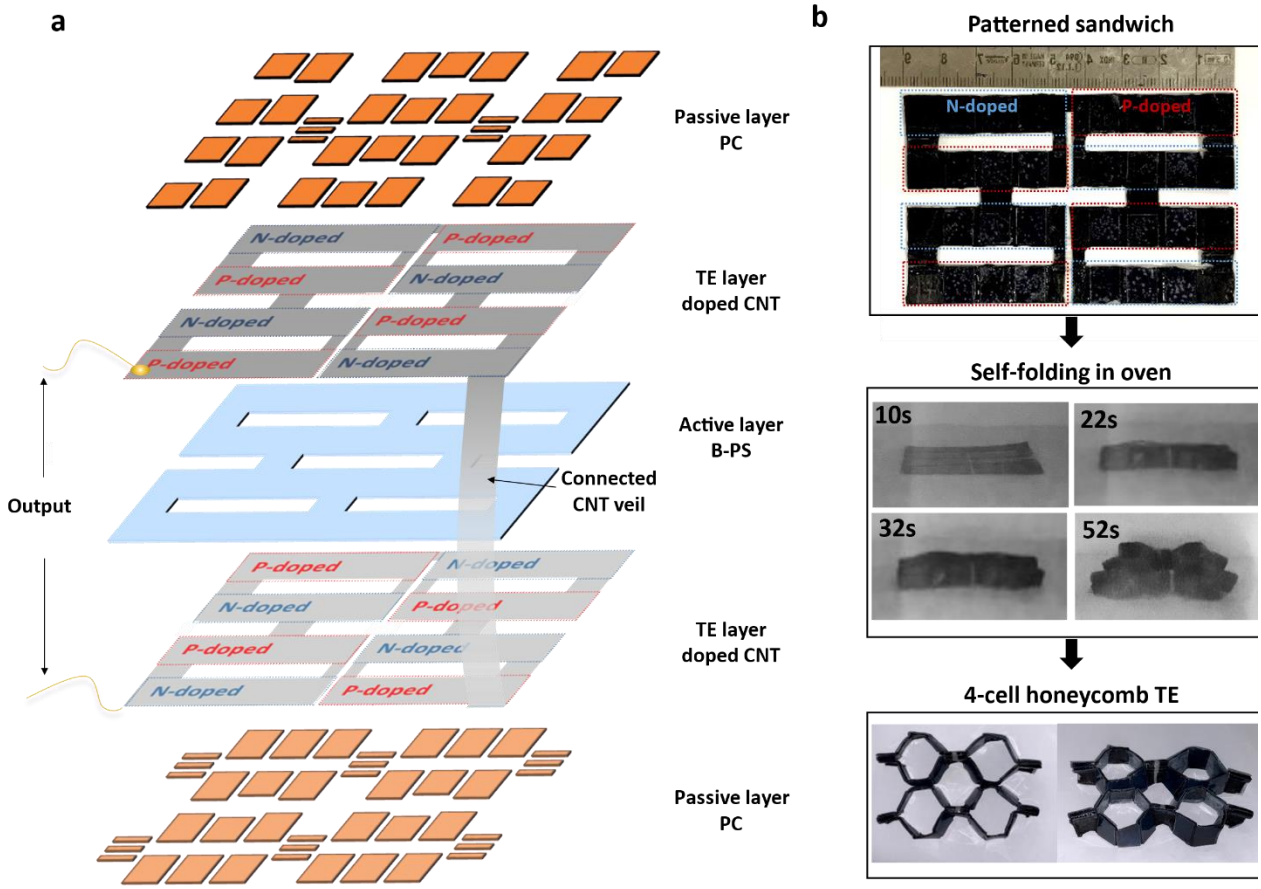

Figure 3. Engineered modular structure of self-folded 4-unit cell honeycomb. (a) Exploded view of the sandwiched honeycomb pattern composed of D2 and D3 patterned PC as passive layer, b-PS as the middle active layer and tailored p&n-type doped CNT veils as interlayer for TE property. (b) Images of the fabrication process of the TE module with 4-unit cell honeycomb structure via self-folding processes.

3.3 Thermoelectric performance of self-folded CNT honeycomb modular structures

To evaluate the thermoelectric performance and power output of the fabricated CNT honeycombs, the single unit cell consists of one pair of p-n legs has been examined under various temperature difference at out-of-plane direction (**Figure 4a**). Under a $\Delta T \sim 20$ ºC, a single pair of

the p-n legs can generate a voltage of 2.5mV with a peak power output up to 115 nW (**Figure 4b**), which is already higher than most reported values from CNT-based TE modules in the literature [3, 32]. Theoretically, an increasing number of the thermocouples (n) can increase both the voltage output U and the maximum power output P_{max}. Therefore, the energy harvesting performance of the 4-unit cell TE module has also been examined to demonstrate the potential of further enhancing the output power by increasing the number of thermocouples in series. As shown in the following equations, the maximum power output should be obtained when the externally loaded resistance is equal to the sum of internal resistance (R_i) of the TE module and contact resistance (R_c).

$$U = n(\alpha_p + \alpha_n)\Delta T \qquad \textbf{Equation (1)}$$

$$P_{max} = \frac{U^2}{4(R_i+R_c)} \qquad \textbf{Equation (2)}$$

where α_p and α_n refer to the absolute values of Seebeck coefficient of the p and n doped CNT veils, which are 60 μV K^{-1} and 69 μV K^{-1}, respectively. Therefore, under a constant temperature difference (ΔT) the $U \propto n$. Meanwhile, the internal resistance is also increasing linearly with the number of thermocouples due to the increased number of series connected of CNT electrodes. Thus, for a TE module with a large number of the thermocouples, R_i should be much higher than R_c, and increases linearly with the number of thermocouples since the average resistance per p-n pair is nearly constant, while the P_{max} should be proportional to n.

The measured power output in **Figure 4c** is in good agreement with this relationship. The highest voltage generated by the four cells honeycomb structure with eight thermocouples was around 21 mV, together with a maximum power output of 812 nW under 17 °C temperature difference, exceeding the reported values in composites from literature with a much lower temperature difference [15]. These values are around 8 times of the energy harvesting capability from the single unit thermocouples, which are in consistent with reported literature in boosting power output by

increasing numbers of paired p-n legs [33]. The output power density of the 4-unit cell TE device is 6940 mW g^{-1} (for pure CNT veils without polymer layers) at per temperature difference squared ΔT^2, with detailed calculation show in **SI Section 3** and comparison in **Table 2**. Obviously, both the voltage output and power output can be further increased with increasing numbers of unit cells in current honeycomb structured TE module. Based on current relationship between numbers of connected thermocouples and obtained power output, 10 μW can be achieved in honeycomb TE module consisting of 50-unit cell (100 effective thermocouples) at a temperature difference of 17 ºC only, fulfilling the practical requirements of many electronics and devices. Besides, the durability of the self-folded TE module after more than 3 years under atmosphere were also reported in **Figure S12**. The 4-thermocouple structured TE module still can provide 4mV voltage output with peak power output of 40 nW under 14 ºC temperature difference.

Table 2. TE property summary of the CNT based TE generators

Device	**p&n pairs**	**Power output ($\mu W\ m^{-1}\ K^{-2}$)**	**Power density normalized by area ($\mu W\ m^{-2}\ K^{-2}$)**	**Power density normalized by weight ($\mu W\ g^{-1}\ K^{-2}$)**	**Ref**
This work	8	21mV and 812 nW at ΔT~17K	2.82	6940 (CNT veils only) 0.0115 (four-cell device with polymer layers)*	
Doped CNT fibres wrapped with acrylic fibres	15	70mWm^{-2} at ΔT~44 K	35	-	[21]
Au-doped CNT webs	7	1.74 μW at ΔT~20 K	10	1.4	[22]
$NaBH_4$ doped CNT film	1	6 mV, 25 nW at ΔT~ 22K	0.0001	-	[23]

CNT yarns	60	10.85 μW g^{-1} at dT~ 5K 697 μW g^{-1} at dT~40 K	-	2.17	[11]
Single-walled CNT buckypapers	37.5	10.3 μW at ΔT~ 30 K.	0.15	-	[26]
Carbon fiber composites	10	20mV, 50 μW at ΔT~ 75 K	0.00025	-	[15]
PEDOT:PSS/CNT composite yarn	966	171.7 μW/(g·K) at ΔT~47.5 K	22.8	3.6	[27]
CNT fiber	40	15.4 μW g^{-1} at ΔT~5K 259 μW g^{-1} at ΔT~20 K	-	3.08	[28]
CNT fiber	72	150 mV; 31 μW at ΔT~32K	0.002	-	[29]
CNT fibric	10	2.3 mV ΔT~5K	23	-	[30]

*the weight of PC and PS films in four-cell device is estimated to be 0.24g.

Additionally, the existence of a large number of cavities within the honeycomb structure also brings benefits of a low thermal diffusion coefficient at out-of-plane direction, maintaining a stable temperature difference without the needs of an external cooling system. As shown in **Figure 4d**, the temperature gradients across the 4-unit cell honeycomb TE module were very stable, regardless of the use of a cooling system on the opposite surface. After reaching the thermal equilibrium of the TE module with a bottom heating pad set at 90 ºC, the temperature of the cold side was 47 ºC without active cooling, translating to a ΔT ~ 43 ºC across the TE module. Compared to the system

with cooling system set at the top (ΔT ~ 50 ºC), only 14% temperature loss was observed, thanks to the cavities within these honeycomb structures.

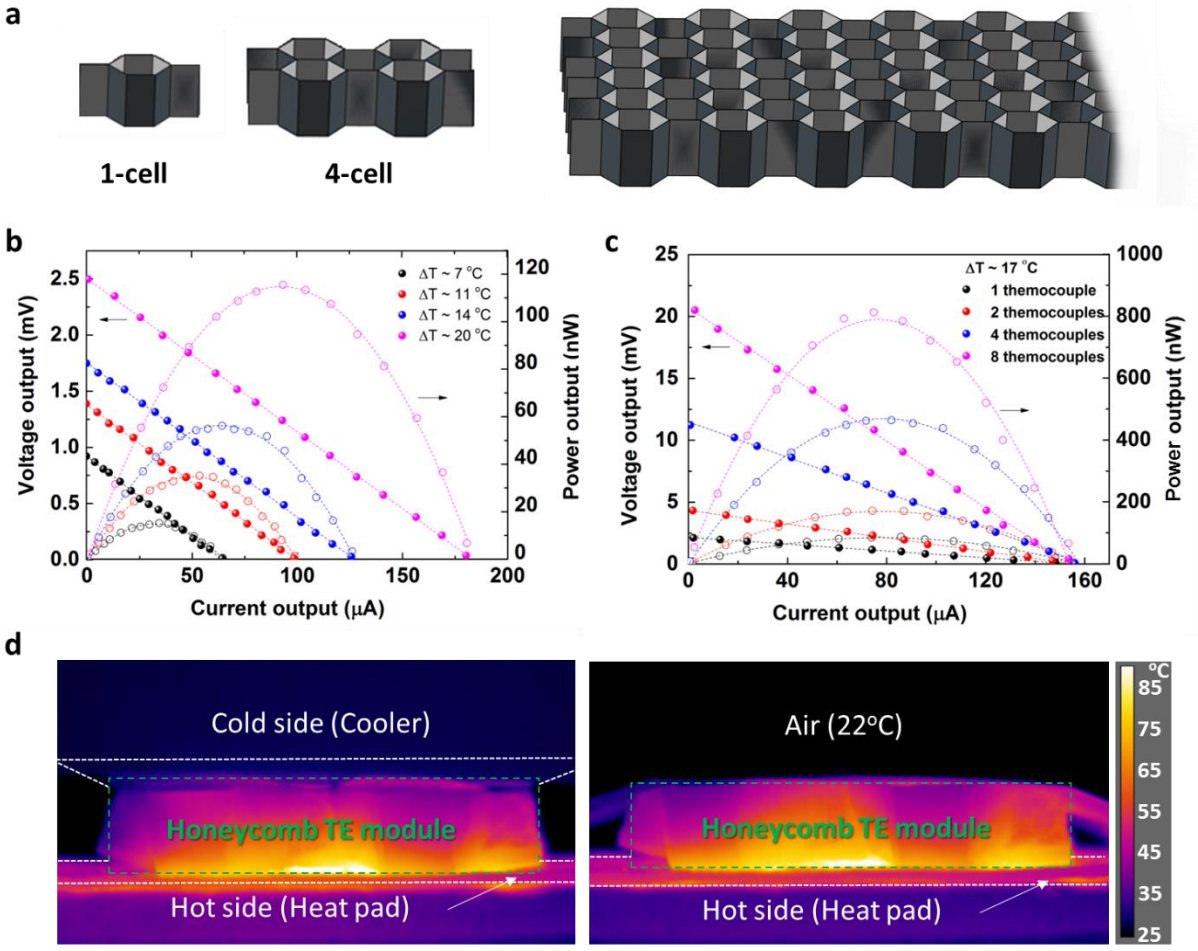

Figure 4. TE performance of CNT honeycomb structures. (a) The schematic illustrations of the self-folded single unit cell, four-cell and multi-cells honeycomb structured TE modules; (b) The voltage and power output from single-unit cell honeycomb TE module consists of a single thermal couple at various temperature differences, with peak output of 2.5mV and 115nW at ΔT ~ 20 ºC; (c) The voltage and power output from different numbers of thermocouples, with the peak output of 21mV and 812nW from the four-unit cell (8 thermocouples) honeycomb TE module at

ΔT ~ 17 ºC; (d) Thermal images of the cross-sectional views of the four-unit cell honeycomb TE module, confirming a stable thermal gradients regardless of an active cooling at the top surface.

3.4 Self-powered strain and damage sensing in high performance composite laminates

The fabricated honeycomb TE modules can be integrated into composite laminates, adding multifunctionalities such as *in-situ* sensing to the components in two different ways: either as a self-powered sensor by harvesting thermal energy to detect the deformation and damage, or as a temperature sensor to monitor the external temperature variations by measuring the power output generated from thermoelectric effect.

Since the electrical sensing method is utilised for deformation and damage monitoring in multifunctional composites, prior to examining the self-powered sensing capabilities based on the honeycomb TE module, the electrical sensing performance with an external power supply has been evaluated first for current system. The nano-engineered hierarchical composites consist of glass fiber reinforced plastics (GFRPs) with a thin layer of percolated CNT sensory network spray coated at the top ply as the sensing layer is used here[19, 34], with the resistance measured as the sensing signals throughout the flexural tests (**Figure 5a**). Morphological observations show a good quality of the laminates without any obvious voids (Figure 5b). Upon loading, although matrix cracking and interfacial debonding can be expected at relatively low strains (as evidenced in Figure 5c), the electrical sensing signals remained almost unchanged at the beginning of the test (Figure 5d). This is due to the limited deformation and damage of the sensing layers at the outer layer of the laminates, especially considering the local high CNT loading which is well above the percolation threshold. With the damages accumulated within the laminates and propagated to delamination and fiber breakages, obvious changes in the load curve can be found with clear load

drops (annotated i within **Figure 5d**), indicating irreversible damages within the specimen. However, due to the relatively high amount of CNTs employed in the sensing layer, no obvious electrical sensing signals can be observed until the cracks have progressed with obvious damage at the outer sensing layer (annotated ii in **Figure 5d**), showing obvious jumps in electrical sensing signals. Clear sensing signals can be found with the damage propagating within the sensing layers, with reduced loading levels observed from the load-displacement curve. Although the sensitivity can be adjusted and improved by reducing the amount of CNTs towards the percolation threshold, high initial electrical conductivity might be required for certain applications therefore at the costs of sensitivity in current sensing method.

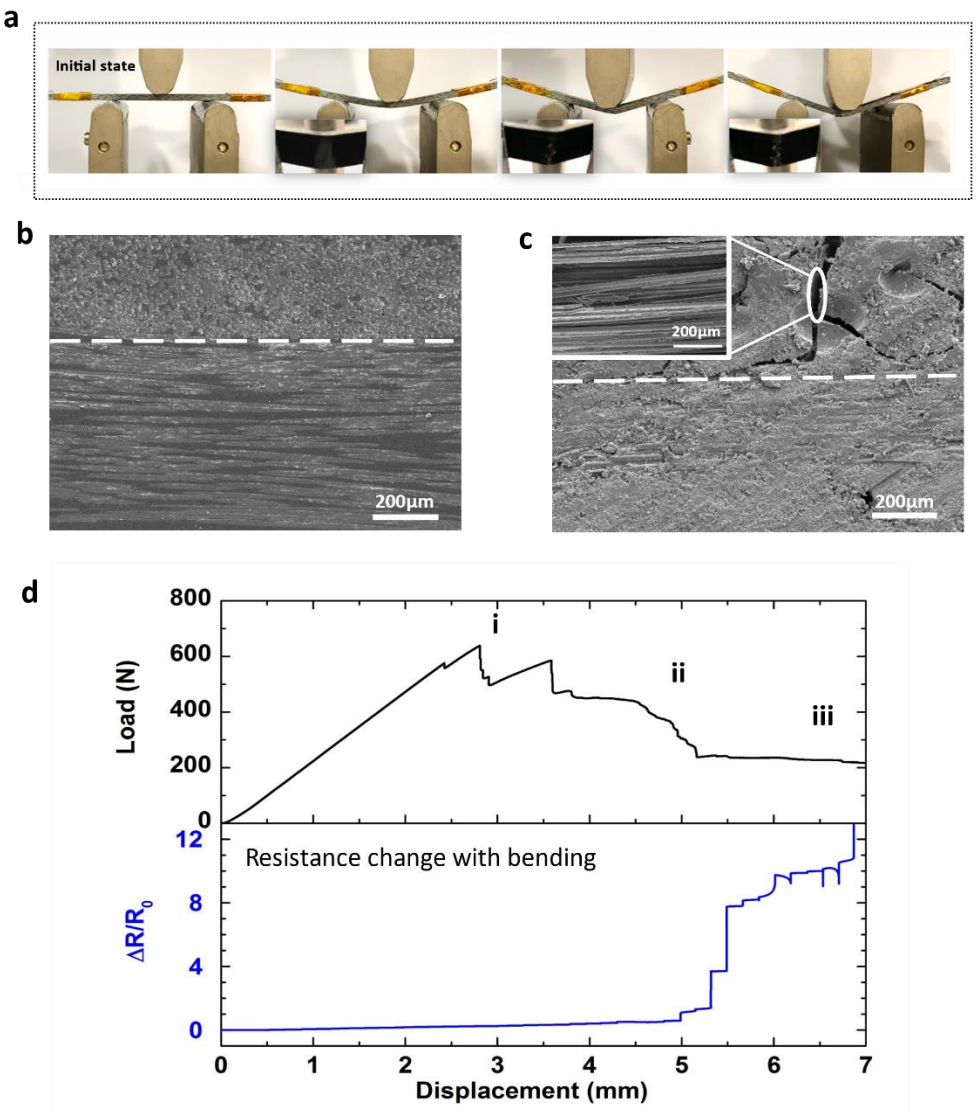

Figure 5. ***In-situ*** **sensing in composite laminates under flexural loadings**: (a) photos taken from three-point bending tests at different stages of the test; SEM images of the cross-sectional views of the nano-engineered hierarchical composites consist of glass fiber/epoxy with a thin layer of percolated CNT spray coated at the top ply (b) before and (c) after three point bending test. (d) electrical resistance sensing based on external power supply, showing clear sensing signals when the damage propagated to the surface sensing layer.

Instead of relying on external power supply, the current output generated via thermal energy harvesting can also be utilized to develop a self-powered sensing system (**Figure 6a**). The thermoelectric (TE) module can reach a stable temperature gradient in ~5min with a temperature difference of ~20 ºC between top and bottom sides (**Figure 6b&c**). Under a constant temperature difference, the voltage output generated from the TE module will remain constant. Therefore, any change in electrical resistance from the sensing layer will lead to a change in the current output, which can be utilized as a sensing signal to detect deformation and damage in composite structures.

For the current self-powered sensing method, a stable current output of around 3 μA was achieved with a 17 ºC of temperature difference (**Figure 6d**). Upon flexural loading, the electrical sensing signals remained stable at the very beginning then started to decrease slightly from relatively early stage of the test (around only 1 mm displacement). A gradual decrease in sensing signal can be found, correlating with increased load and deformation of the specimen. This early detection capability can be attributed to the relatively low absolute value of the current output, leading to a high sensitivity at such low strains. With the load continued increasing, delamination and fiber breakage can be expected with clear load drop from the load-displacement curve (annotated i in **Figure 6d**). A further decrease in sensing signals can be found at this stage, regardless of the sensing layer only presented at the outer layer. When the crack propagated and reached outer sensing layer (annotated ii in **Figure 6c**), a very large drop in sensing signals can be found due to the significant change in system resistance value hence the current output. It is worth noting that no external power supply is required for the honeycomb TE module, while the deformation and health conditions with internal damage propagations can be monitored in real time based on thermal energy harvested in this self-powered sensing method.

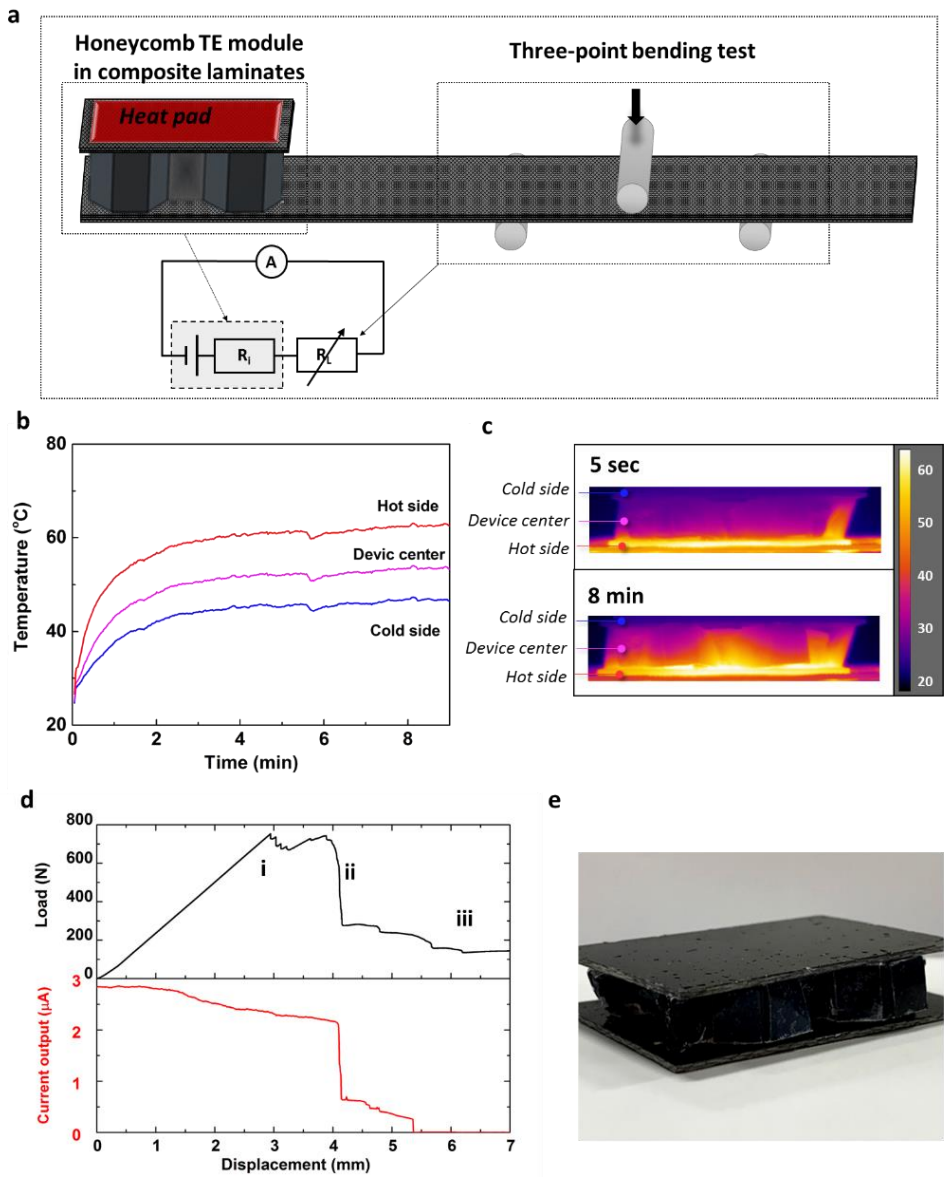

Figure 6. ***In-situ*** **self-powered sensing in composite laminates under flexural loadings.** (a) illustration of current self-powered sensing setup with honeycomb TE module integrated at the side of the specimen; (b) temperature profiles of TE module in contact with a 65ºC heat pad in ambient environment; (c) cross-sectional thermal images of the four-units cell honeycomb TE module at the beginning and stablised temperature condition; (d) self-powered sensing based on thermal energy harvesting (17 ºC), with a clear signal appeared at relatively early stage of the test;

(e) illustration of idealized fully optimised sandwiched structure with CNT honeycomb TE module as the core layer to provide energy harvesting and structural functions.

Clearly, both external powered sensing and self-powered sensing methods can be utilised to monitor the deformation and damage in real time, while the sensitivity can be adjusted depending on the requirements of applications by utilising resistance or current changes as sensing signals. As illustrated in **Figure 6d**, the four-unit cell honeycomb TE module is integrated into the composite laminates but not directly under the flexural loadings during the testing, hence without any effects in mechanical performance. Durability and repeatability of the self-powered sensing property has also been examined with a consistent performance achieved, as shown in the **Figure S12 and S13**. It is worth noting that a fully optimised structure should be developed (**Figure 6e**) with a tailored honeycomb TE structure. The interfacial adhesion needs to be optimised to fulfil a wider range of applications based on current self-folded honeycomb in a sandwiched structural laminate. Nevertheless, this has proved the concepts and provided a feasible strategy to scale-up (and scale-down) the TE device by designing and fabricating a patterned passive layers on the active layers, turning a two dimensional multilayer structure into a three dimensional energy harvesting device at different length scales. A programmable procedure also allows the sequential self-folding with remote triggering of deployable structures, especially for the applications where space is constrained during the transport stage.

4. Conclusions

Self-powered sensing based on thermal energy harvesting has been successfully integrated into a high-performance composite via a temperature induced self-folding process, with capability to

detect deformation and damage in composite laminates without external power supply. Two long lasting issues of using thermal electricity in advanced functional composites have been solved simultaneously, namely (i) harvesting thermal gradient at out-of-plane direction and (ii) generating high power output with a limited temperature difference. High peak outputs of 21mV and 812nW at temperature difference of only 17 ºC has been achieved with a CNT honeycomb structure consists of accurately connected four thermocouples of alternating p-n legs, opening up new routes for self-powered structural health monitoring and thermal energy harvesting in high performance composite applications.

A temperature induced self-folding process has been utilized in this work, turning 1D continues CNT veils into 3D honeycomb structures autonomously upon heating. Various designs have been developed and fabricated to achieve both the modular unit of CNT hexagonal structure as well as the engineered CNT honeycomb structure with accurately connected p-n legs. The thermoelectric properties of continuous CNT veils have been systematically examined and tuned for optimised energy output, with limited effects observed from the self-folding process. A linear relationship between the power output and numbers of TE legs under a constant temperature gradient has been validated with the fabricated CNT honeycomb structures, indicating the power output could reach 10μW with 50-unit cell honeycomb at a temperature of 17 ºC only, which can fulfil the practical requirements of various electronics and devices. The cavities within the honeycomb structure also enabled low thermal diffusion hence facilitated a stable temperature gradient across the specimen without the needs of an active cooling system.

Self-powered sensing based on thermoelectric effects has been successfully achieved in a structural composite laminate, with energy harvested from out-of-plane direction without affecting original performance of the composite laminates. Both elastic deformation and the damage

propagation have been monitored in real time, with sensing signals clearly correlated with various stages of damage upon loading, confirming its great potential to be used as self-powered structural health monitoring system at remote and/or hard to access locations for advanced composite applications.

Supporting Information

Effect of exposure time on the Seebeck coefficient of CNT veils; CNT purification procedures; TGA results, thermoelectric properties, and normalized Raman spectra of the as-grown, annealed, and purified CNT; SEM images of CNT veils; optimization procedures and obtained thermoelectric properties of doped CNT veils; SEM images of doped CTN veils; the self-folding angle with various gap width; comparison between simulation and experimental result on the temperature induced self-folding process; schematic illustrations of the design for 4-cell honeycomb structure TE module; normalized power output calculation; TE performance of the CNT honeycomb structure after 3.5 years; repeated self-powered sensing results.

Acknowledgement

The authors would like to thank the support from the Royal Society (IES\R3\183170, and RGS\R1\211366). K. Wan gratefully acknowledges the financial support from the Chinese Scholarship Council (CSC). JJV is grateful for generous financial support provided by the European Union Horizon 2020 Programme under grant agreement 678565 (ERC-STEM).

References

1. Fernández-Toribio, J. C.; Íñiguez-Rábago, A.; Vilà, J.; González, C.; Ridruejo, Á.; Vilatela, J. J., A Composite Fabrication Sensor Based on Electrochemical Doping of Carbon Nanotube Yarns. *Adv. Funct. Mater.* **2016,** *26* (39), 7139-7147.
2. Iglesias, D.; Senokos, E.; Alemán, B.; Cabana, L.; Navío, C.; Marcilla, R.; Prato, M.; Vilatela, J. J.; Marchesan, S., Gas-Phase Functionalization of Macroscopic Carbon Nanotube Fiber Assemblies: Reaction Control, Electrochemical Properties, and Use for Flexible Supercapacitors. *ACS Applied Materials & Interfaces* **2018,** *10* (6), 5760-5770.
3. Blackburn, J. L.; Ferguson, A. J.; Cho, C.; Grunlan, J. C., Carbon-Nanotube-Based Thermoelectric Materials and Devices. *Adv. Mater.* **2018,** *30* (11), 1704386.
4. Avery, A. D.; Zhou, B. H.; Lee, J.; Lee, E.-S.; Miller, E. M.; Ihly, R.; Wesenberg, D.; Mistry, K. S.; Guillot, S. L.; Zink, B. L.; Kim, Y.-H.; Blackburn, J. L.; Ferguson, A. J., Tailored Semiconducting Carbon Nanotube Networks with Enhanced Thermoelectric Properties. *Nat. Energy.* **2016,** *1*, 16033.
5. Ryu, Y.; Freeman, D.; Yu, C., High Electrical Conductivity and n-type Thermopower from Double-/Single-wall Carbon Nanotubes by Manipulating Charge Interactions between Nanotubes and Organic/Inorganic Nanomaterials. *Carbon* **2011,** *49* (14), 4745-4751.
6. Ebbesen, T. W.; Lezec, H. J.; Hiura, H.; Bennett, J. W.; Ghaemi, H. F.; Thio, T., Electrical Conductivity of Individual Carbon Nanotubes. *Nature* **1996,** *382* (6586), 54-56.
7. Zhou, W.; Fan, Q.; Zhang, Q.; Cai, L.; Li, K.; Gu, X.; Yang, F.; Zhang, N.; Wang, Y.; Liu, H.; Zhou, W.; Xie, S., High-performance and Compact-designed Flexible Thermoelectric Modules enabled by a Reticulate Carbon Nanotube Architecture. *Nat. Commun.* **2017,** *8* (1), 14886.
8. Ou, Y.; González, C.; Vilatela, J. J., Interlaminar Toughening in Structural Carbon Fiber/Epoxy Composites Interleaved with Carbon Nanotube Veils. *Composites Part A: Applied Science and Manufacturing* **2019,** *124*, 105477.
9. Zhou, W.; Fan, Q.; Zhang, Q.; Li, K.; Cai, L.; Gu, X.; Yang, F.; Zhang, N.; Xiao, Z.; Chen, H.; Xiao, S.; Wang, Y.; Liu, H.; Zhou, W.; Xie, S., Ultrahigh-Power-Factor Carbon Nanotubes and an Ingenious Strategy for Thermoelectric Performance Evaluation. *Small* **2016,** *12* (25), 3407-14.
10. An, C. J.; Kang, Y. H.; Song, H.; Jeong, Y.; Cho, S. Y., High-performance Flexible Thermoelectric Generator by Control of Electronic Structure of Directly Spun Carbon Nanotube Webs with Various Molecular Dopants. *Journal of Materials Chemistry A* **2017,** *5* (30), 15631-15639.
11. Choi, J.; Jung, Y.; Yang, S. J.; Oh, J. Y.; Oh, J.; Jo, K.; Son, J. G.; Moon, S. E.; Park, C. R.; Kim, H., Flexible and Robust Thermoelectric Generators Based on All-Carbon Nanotube Yarn without Metal Electrodes. *ACS Nano* **2017,** *11* (8), 7608-7614.
12. Choi, J.; Jung, Y.; Dun, C.; Park, K. T.; Gordon, M. P.; Haas, K.; Yuan, P.; Kim, H.; Park, C. R.; Urban, J. J., High-Performance, Wearable Thermoelectric Generator Based on a Highly Aligned Carbon Nanotube Sheet. *ACS Applied Energy Materials* **2020,** *3* (1), 1199-1206.
13. Karalis, G.; Tzounis, L.; Tsirka, K.; Mytafides, C. K.; Voudouris Itskaras, A.; Liebscher, M.; Lambrou, E.; Gergidis, L. N.; Barkoula, N.-M.; Paipetis, A. S., Advanced Glass Fiber Polymer Composite Laminate Operating as a Thermoelectric Generator: A Structural Device for Micropower Generation and Potential Large-Scale Thermal Energy Harvesting. *ACS Applied Materials & Interfaces* **2021,** *13* (20), 24138-24153.
14. Karalis, G.; Tzounis, L.; Tsirka, K.; Mytafides, C. K.; Liebscher, M.; Paipetis, A. S., Carbon Fiber/Epoxy Composite Laminates as Through-thickness Thermoelectric Generators. *Composites Science and Technology* **2022,** *220*, 109291.

15. Karalis, G.; Tzounis, L.; Lambrou, E.; Gergidis, L. N.; Paipetis, A. S., A Carbon Fiber Thermoelectric Generator Integrated as a Lamina within an 8-ply Laminate Epoxy Composite: Efficient Thermal Energy Harvesting by Advanced Structural Materials. *Applied Energy* **2019,** *253*, 113512.
16. Xu, H.; Tong, X.; Zhang, Y.; Li, Q.; Lu, W., Mechanical and Electrical Properties of Laminated Composites containing Continuous Carbon Nanotube Film Interleaves. *Composites Science and Technology* **2016,** *127*, 113-118.
17. Xu, X.; Zhang, Y.; Jiang, J.; Wang, H.; Zhao, X.; Li, Q.; Lu, W., In-situ Curing of Glass Fiber Reinforced Polymer Composites via Resistive Heating of Carbon Nanotube Films. *Composites Science and Technology* **2017,** *149*, 20-27.
18. Zhang, H.; Kuwata, M.; Bilotti, E.; Peijs, T., Integrated Damage Sensing in Fibre-reinforced Composites with Extremely Low Carbon Nanotube Loadings. *Journal of Nanomaterials* **2015,** *2015* (Article ID 785834), 7.
19. Zhang, H.; Liu, Y.; Kuwata, M.; Bilotti, E.; Peijs, T., Improved Fracture Toughness and Integrated Damage Sensing Capability by Spray Coated CNTs on Carbon Fibre Prepreg. *Composites Part a-Applied Science and Manufacturing* **2015,** *70*, 102-110.
20. Bradley, K.; Jhi, S.-H.; Collins, P. G.; Hone, J.; Cohen, M. L.; Louie, S. G.; Zettl, A., Is the Intrinsic Thermoelectric Power of Carbon Nanotubes Positive? *Phys. Rev. Lett.* **2000,** *85* (20), 4361-4364.
21. Sun, T.; Zhou, B.; Zheng, Q.; Wang, L.; Jiang, W.; Snyder, G. J., Stretchable fabric generates electric power from woven thermoelectric fibers. *Nat. Commun.* **2020,** *11* (1), 572.
22. An, C. J.; Kang, Y. H.; Lee, A. Y.; Jang, K.-S.; Jeong, Y.; Cho, S. Y., Foldable Thermoelectric Materials: Improvement of the Thermoelectric Performance of Directly Spun CNT Webs by Individual Control of Electrical and Thermal Conductivity. *ACS Applied Materials & Interfaces* **2016,** *8* (34), 22142-22150.
23. Yu, C.; Murali, A.; Choi, K.; Ryu, Y., Air-stable fabric thermoelectric modules made of N- and P-type carbon nanotubes. *Energy & Environmental Science* **2012,** *5* (11), 9481-9486.
24. Yu, C.; Choi, K.; Yin, L.; Grunlan, J. C., Light-weight Flexible Carbon Nanotube based Organic Composites with Large Thermoelectric Power Factors. *ACS nano* **2011,** *5* (10), 7885-7892.
25. Zhao, X.; Han, W.; Jiang, Y.; Zhao, C.; Ji, X.; Kong, F.; Xu, W.; Zhang, X., A Honeycomb-like Paper-based Thermoelectric Generator based on a Bi2Te3/bacterial Cellulose Nanofiber coating. *Nanoscale* **2019,** *11* (38), 17725-17735.
26. Kim, S.; Mo, J.-H.; Jang, K.-S., Solution-Processed Carbon Nanotube Buckypapers for Foldable Thermoelectric Generators. *ACS Applied Materials & Interfaces* **2019,** *11* (39), 35675-35682.
27. Zheng, Y.; Zhang, Q.; Jin, W.; Jing, Y.; Chen, X.; Han, X.; Bao, Q.; Liu, Y.; Wang, X.; Wang, S.; Qiu, Y.; Di, C.-a.; Zhang, K., Carbon Nanotube Yarn Based Thermoelectric Textiles For Harvesting Thermal Energy And Powering Electronics. *Journal of Materials Chemistry A* **2020,** *8* (6), 2984-2994.
28. Lee, T.; Park, K. T.; Ku, B.-C.; Kim, H., Carbon Nanotube Fibers with Enhanced Longitudinal Carrier Mobility for High-performance All-carbon Thermoelectric Generators. *Nanoscale* **2019,** *11* (36), 16919-16927.
29. Kim, S. L.; Choi, K.; Tazebay, A.; Yu, C., Flexible Power Fabrics Made of Carbon Nanotubes for Harvesting Thermoelectricity. *ACS Nano* **2014,** *8* (3), 2377-2386.

30. Ito, M.; Koizumi, T.; Kojima, H.; Saito, T.; Nakamura, M., From Materials to Device Design of a Thermoelectric Fabric for Wearable Energy Harvesters. *Journal of Materials Chemistry A* **2017,** *5* (24), 12068-12072.
31. Kernin, A.; Ventura, L.; Soul, A.; Chen, K.; Wan, K.; Lu, W.; Steiner, P.; Kocabas, C.; Papageorgiou, D.; Goutianos, S.; Zhang, H.; Bilotti, E., Kirigami Inspired Shape Programmable and Reconfigurable Multifunctional Nanocomposites for 3D Structures. *Materials & Design* **2022,** *224*, 111335.
32. Zhang, Y.; Heo, Y.-J.; Park, M.; Park, S.-J., Recent Advances in Organic Thermoelectric Materials: Principle Mechanisms and Emerging Carbon-based Green Energy Materials. *Polymers* **2019,** *11* (1), 167.
33. Wan, K.; Taroni, P. J.; Liu, Z.; Liu, Y.; Tu, Y.; Santagiuliana, G.; Hsia, I.-C.; Zhang, H.; Fenwick, O.; Krause, S.; Baxendale, M.; Schroeder, B. C.; Bilotti, E., Flexible and Stretchable Self-Powered Multi-Sensors Based on the N-Type Thermoelectric Response of Polyurethane/Nax(Ni-ett)n Composites. *Adv. Electron. Mater.* **2019,** *5* (12), 1900582.
34. Zhang, H.; Liu, Y.; Bilotti, E.; Peijs, T., In-Situ Monitoring of Interlaminar Shear Damage in Carbon Fibre Composites. *Advanced Composites Letters* **2015,** *24* (4), doi:10.1177/096369351502400405.

Table of Contents